

Development of large grain cavities

W. Singer,* S. Aderhold, A. Ermakov, J. Iversen, D. Kostin, G. Kreps, A. Matheisen,
W.-D. Möller, D. Reschke, X. Singer, K. Twarowski, and H. Weise
Deutsches Elektronen-Synchrotron DESY, Notkestrasse 85, DE-22603 Hamburg, Germany

H.-G. Brokmeier

Technische Universität Clausthal, Institut für Werkstoffkunde und Werkstofftechnik, 38678 Clausthal-Zellerfeld, Germany
(Received 29 November 2011; revised manuscript received 27 November 2012; published 15 January 2013)

DESY activities on 1.3 GHz tesla shape single cell and nine-cell large grain (LG) resonators are presented; results of the past five years are covered. The R&D program explores the potential for production of elliptical superconducting cavities. The main efforts have been devoted to material investigation, development of LG disk production, cavity fabrication from this material, and a search for appropriate treatment. More than 250 LG disks are manufactured; several single cell and 11 nine-cell resonators are produced and rf tested after buffered chemical polishing and after additional electropolishing. A maximum accelerating gradient of approximately 45 MV/m for this type of cavity was achieved in two resonators. Two of the LG cavities have been installed and are currently being used in the FLASH accelerator operation. Assembly of a cryomodule, consisting of LG cavities only, is in the works. Perspectives of the LG cavity application are discussed.

DOI: [10.1103/PhysRevSTAB.16.012003](https://doi.org/10.1103/PhysRevSTAB.16.012003)

PACS numbers: 41.60.Cr

I. INTRODUCTION

The manufacturing approach for producing the cavities by deep drawing and electron beam welding using disks cut from electron beam melted ingot [large grain (LG) cavities] has worldwide interest [1,2]. This option, which allows the elimination of the long production chain from large grain ingot to fine grain sheet, has been proposed at Jefferson Lab and Companhia Brasileira de Metalurgia e Mineração (CBMM) [3–5]. Very promising performance with accelerating gradients up to 35 MV/m, reached by buffered chemical polishing (BCP) treatment only, was demonstrated on single cell cavities.

Several aspects were investigated in the scope of the DESY R&D program of LG resonators. One of the aspects was the material issue: what are the advantages and disadvantages of LG compared to fine grain (FG) material; can a significant amount of LG niobium be produced by industry in a cost effective manner. The second issue was the fabrication of cavities: could the series production of resonators be done on the level of required tolerances. Third was the performance issue: what will be the highest achieved accelerating gradient, what is the appropriate treatment for achieving a stable and reproducible gradient, do LG cavities have advantages compared to conventional FG cavities.

*waldemar.singer@desy.de

Published by the American Physical Society under the terms of the *Creative Commons Attribution 3.0 License*. Further distribution of this work must maintain attribution to the author(s) and the published article's title, journal citation, and DOI.

II. MATERIAL

A. LG Material production

Development of the LG disk production was done within the framework of the R&D program of DESY and W. C. HERAEUS in 2007–2008 [6].

One of the issues to be solved was efficient cutting of the disks. W. C. HERAEUS developed a wire saw cutting procedure that seems to be cost effective, assuming that the company can do the slicing of many tens of disks simultaneously while keeping the material purity high ($RRR > 300$) and achieving tight thickness tolerances (better than ± 0.1 mm) (see Fig. 1) and high surface quality ($Ra < 1.6$).

A similar procedure was also developed at the Tokyo Denkai company later [7].

Another DESY requirement, to assure the presence of a single crystal with a diameter larger than 150 mm in the disk's central area, was also fulfilled by the company. On one hand, this requirement is essential for avoiding

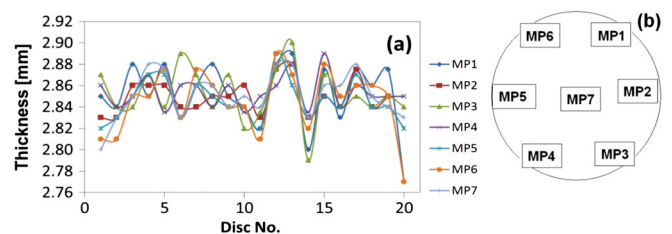


FIG. 1. Thickness distribution (a) and measurement locations (b) in the LG disks of the W. C. HERAEUS with approximately 300 mm diameter. Tolerances are more narrow than those required by the XFEL Specification (2.8 ± 0.1 mm).

possible necking and tearing at the irises during deep drawing (see below); on the other hand, it should reduce the field emission in the area vulnerable to field emission, due to absence of the grain boundary steps close to the iris.

About 250 large grain niobium disks with RRR = 320–500 have been delivered to DESY.

It can be expected that the disk material from ingots is less sensitive to contamination by foreign material or other types of defects, because it is taken directly from homogeneous ingot material that has been very slowly remelted many times. Several types of flaws (delamination, imbedded particles, oxides, etc.) which can occur during forging or rolling are avoided in this case. The disks used for manufacturing of the first three cavities numbered AC112–AC114 have been scanned by the eddy current device available at DESY [8]. No indications of localized defects in the crystals were observed. Therefore, it was decided not to scan the disks provided for the next eight LG cavities.

B. LG Material properties: Characterization of the crystals in LG disks

The crystallographic structure of major large grains of three Nb disks with diameter 200–300 mm of vendors W. C. HERAEUS, CBMM, and Ningxia was investigated with the aim to find out whether the large grains (that have the dimensions of several tens of mm) are really single crystals. Measurements of crystal reflexes were done at DESY HASYLAB [8]. These experiments have been done by complete penetration of x ray, unlike conventional x-ray diffraction, which allows only surface crystallographic analysis.

The W. C. HERAEUS disk (of 270 mm diameter) consists of a big central crystal (> 150 mm cross section) and some smaller edge crystals [Figs. 2(a) and 2(b)]. Figure 2(b) represents the superimposition of five measured locations (1–4; 10) on the central crystal, which confirms the high quality of single crystal (weakly pronounced mosaic structure). The edge crystals (single crystals of high quality too) show distinctly different orientations compared to the central crystal.

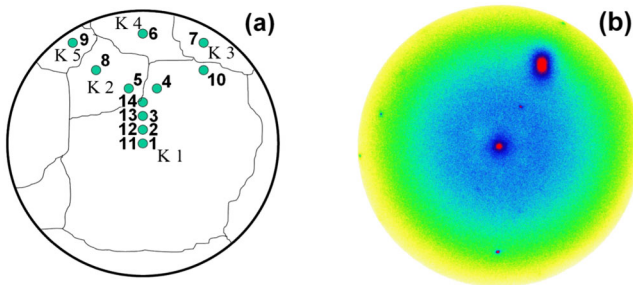


FIG. 2. (a) LG distribution in the W. C. HERAEUS disk and measurement locations. (b) X-ray reflexes on the central crystal of the W. C. HERAEUS disk.

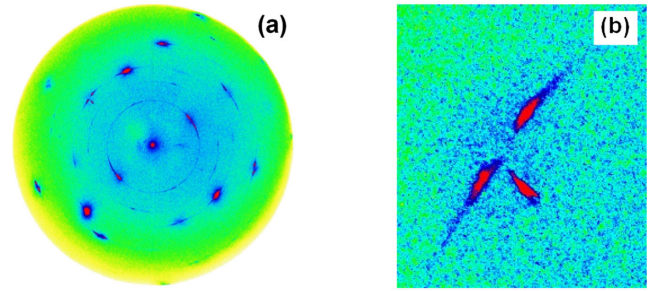


FIG. 3. (a) Example of Debye Scherrer rings as an indication for the small crystals in the LG disk of Ningxia OTIC company's ingot. (b) Signal splitting of reflexes in the LG disk of Ningxia OTIC company's ingot.

The central crystal of the CBMM ingot possessed very large homogeneity too. Measurement in seven different locations of the central crystal has shown very small fluctuations proving high quality of the single crystal. The edge crystals create many small single crystals and subcrystals.

The Ningxia OTIC disk had many crystals [Figs. 3(a) and 3(b)] with a wide scattering of orientations. In a disk center, a splitting of reflexes (indication for several single crystals) and Debye Scherrer rings (indication for the powder or small crystals material) was clearly observed in addition to the strong single crystal signal.

C. Material properties: Thermal conductivity of large grain niobium

LG cavities have a smaller number of grain boundaries compared to fine grain material. A maximum in thermal conductivity “phonon peak” near the accelerator's operation temperature of 2 K could be expected in this case due to diminishing of scattering of phonons on a smaller number of grain boundaries. The LG cavities could benefit from this phenomena.

The thermal conductivity of large grain niobium samples (with or without grain boundaries) measured at low temperatures is compared to fine grain in Fig. 4 (see also [9]). The experimental results demonstrate a pronounced phonon peak on large grain samples of the W. C. HERAEUS company heat treated at 800°C, while no phonon peak is observed on fine grain samples independently on the RRR value. The dependence of the phonon peak on crystallographic orientation is not detected. A phonon peak was not observed on a large grain niobium sample from Ningxia OTIC company possibly because Ningxia OTIC large grains consist of many smaller powderlike crystals (see above).

The theory of thermal conductivity in the superconducting state is rather complicated. The total heat conductivity of the superconducting metal is a sum of electron and phonon terms. In the superconducting state the electron contribution decreases essentially because of the electrons

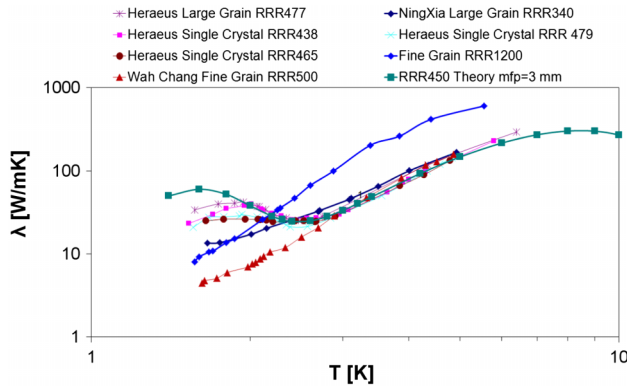


FIG. 4. Thermal conductivity of fine grain, large grain, and single crystal niobium (mfp: phonon mean-free path).

binding into Cooper pairs. A fraction of electrons contributes to heat transport, but this contribution reduces very rapidly with temperature decreasing. The phonon part is usually negligible for metals compared to the electron contribution. However, in the superconducting state, due to small electron heat conduction at temperatures below $T/T_c = 0.3$, the phonon portion of the total thermal conductivity becomes significant.

An empirical expression for quantitative estimation of the thermal conductivity of niobium at low temperatures was proposed in the work [10], Eq. (1):

$$\lambda(T) = R(y) \left[\frac{\rho_{295K}}{L_0 \cdot \text{RRR} \cdot T} + aT^2 \right]^{-1} + \left[\frac{1}{D \exp(y)T^2} + \frac{1}{BIT^3} \right]^{-1}, \quad (1)$$

where T is temperature, RRR is residual resistivity ratio, l is phonon mean-free path.

The fitting coefficients regarding high purity niobium are given in work [10]: $y = \alpha T_c/T$, T_c is the critical temperature of Nb, $\alpha = 1.76$, $L = 2.45 \times 10^{-8} \text{ WK}^{-2}$, $a = 2.3 \times 10^{-5} \text{ mW}^{-1} \text{ K}^{-1}$, $1/D = 300 \text{ mK}^{-3} \text{ W}^{-1}$, $B = 7.0 \times 10^3 \text{ Wm}^{-2} \text{ K}^{-4}$. $R(y)$ can be roughly fitted as

$$R(y) = -0.28401y^3 + 4.6281y^2 + 0.7787y - 0.0131.$$

The first part in brackets of (1) describes the scattering of electrons on impurities, lattice defects, and scattering of electrons on phonons. The second part in brackets describes the scattering of phonons on electrons and scattering of phonons on grain boundaries.

Calculation of thermal conductivity using the formula for $\lambda(T)$ and the sample width of approximately 3 mm (instead of grain size for polycrystalline material normally approximately $50 \mu\text{m}$) as the phonon mean-free path can be seen in Fig. 4. Indeed the phonon peak is clearly seen.

Further investigation of thermal conductivity showed that even a rather small plastic deformation of 8.5% makes the phonon peak totally disappear (Fig. 5). A similar result was also observed in [11] on niobium single crystals. The

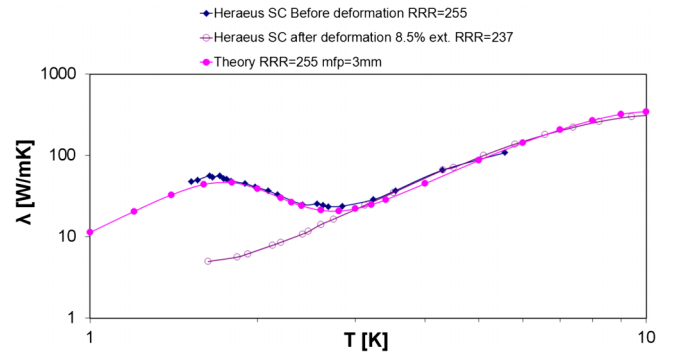


FIG. 5. Plastic deformation influence on thermal conductivity of single crystal niobium.

phonon peak rises again after recovery annealing at 800°C for 2 h [12]. It implies that the large grain cavity might not benefit from the thermal conductivity enhancement due to the plastic deformation during cavity fabrication (deep drawing). Therefore final annealing at approximately 800°C is required not only for outgassing of the hydrogen but also for the stress relaxation.

D. Mechanical properties: Tensile test; bulge test

The crystallographic orientation of LG niobium samples used for the tensile and bulging tests can be seen in Fig. 6. Uniaxial tensile tests were performed on three differently oriented Nb large grain samples. The results of stress dependence on the percentage elongation $\sigma(\Delta l/l)$ demonstrate rather high elongation at break values, comparable with the highest values of fine grain material (up to 70%). In addition, a significant anisotropy of the elongation at break from approximately 55% up to approximately 110% (Fig. 7) that depends evidently on the positioning of the long axis of the sample and crystal orientation was observed.

A hydraulic bulge test [13] was conducted to evaluate the biaxial LG niobium properties and to compare with the uniaxial tensile test. Figure 8 shows the scheme of DESY bulge test equipment. This method allows getting the true strain-stress characteristic of the material.

During the test, a disk with 130 mm diameter is bulged into a die with 100 mm inner diameter. Figure 9 shows the results of biaxial bulge tests. Elongation ε after fracture by

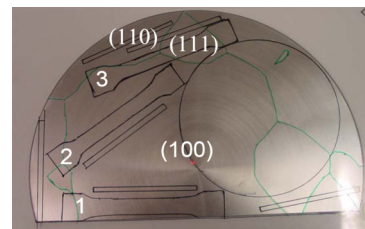


FIG. 6. Samples positioned in the LG disk for tensile and bulge tests.

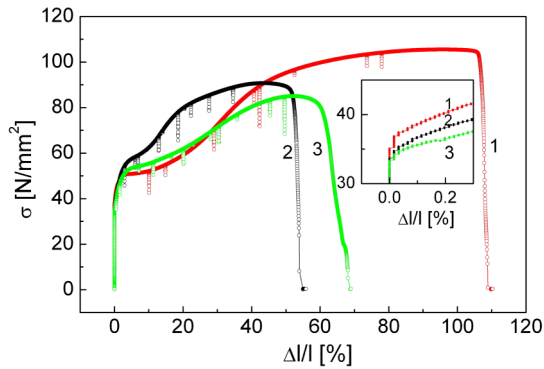


FIG. 7. Tensile tests results for three LG samples cut according to Fig. 6.

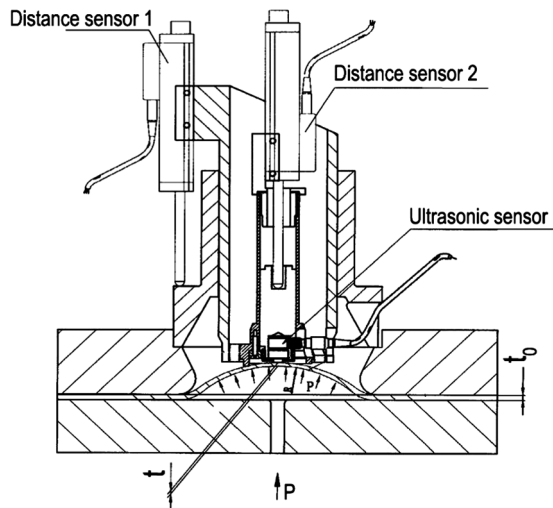


FIG. 8. Scheme of the bulge test device.

biaxial deformation for large grain is approximately 12% and significantly lower compared to tensile test results. The rupture takes place on the grain boundary close to the center of the disk.

The bulge test allows us to draw the conclusion that despite high elongation values observed in the tensile test

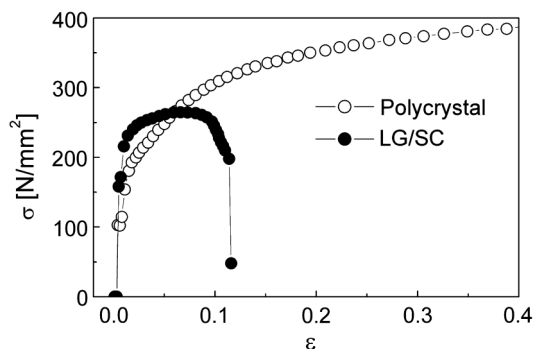


FIG. 9. Biaxial bulge test results on a large grain Nb sample. The curve for the polycrystalline sample is shown as reference.

the LG material is frail to biaxial deformations like deep drawing of half-cells, for example. During the deep drawing the maximal plastic deformation is approximately 15%. This means that the areas of the highest deformation degree like the iris can be critical for ruptures at grain boundaries. Such ruptures were in fact observed in some cases. This is why, in order to ensure a reliable deep drawing, the requirement of the presence of a single crystal with a diameter larger than 150 mm was included in DESY's specifications for LG material.

III. FABRICATION

The following single cell cavities were produced using W.C. HERAEUS ingot material: 1AC3, 1AC4, 1AC5, 1AC7, 1DE20, and 1DE21. In addition, two LG single cell cavities 1DE25 and 1DE26 were built from ingots of the CBMM Company (Brazil). Machining, etching, electron beam welding, and mechanical/optical quality control was done in-house for some of the single cell cavities [14].

Six single cell cavities and 11 nine-cell LG cavities AC112–AC114, AC151–AC158 of tesla shape were produced at ACCEL Instruments GmbH (now Research Instrument GmbH RI), from W.C. HERAEUS material.

Deep drawing of the half-cells was done using the same tools as for fine grain material. The grain boundaries were noticeably pronounced with steps up to 0.5 mm. In two cavities, AC155 and AC156, the steps on grain boundaries were ground away with the intention to compare the performance of ground and nonground cavities. Tactile 3D measurement at RI and optical coordinate measurement with 3D imaging at company DECOM was done in order to estimate the shape accuracy.

The deep drawn half-cells have, sometimes, a quadrangular or oval shape and do not meet the required tolerance of ± 0.2 mm. The half-cells' shape deviation for cavities AC151–AC153 was more pronounced compared to cavities AC154–AC158 (see Fig. 10). It turned out that the orientation of the large central crystals in the disks had a big influence on the shaping. Analysis of the crystal orientation done with the Lauer technique showed that for disks of AC151–AC153, the main orientation of the central crystal is (100), and for disks of AC154–AC158, it was mainly (211) or (221). It is well known that the main atom plane slipping for body centered cubic metals takes place in the (110) planes in the [111] direction; therefore, for the disks with (100) orientation, a more pronounced anisotropy and quadrangular shape after deep drawing should be expected in agreement with observations.

The pronounced shape deviation in the half-cells generated some difficulties for assembly of half-cells and especially of dumbbells for welding. RI overcomes these difficulties by using a special tool that ensures precise assembly of the male and female half-cells together. Applying the DESY length adjustment procedure [15] allowed us to achieve the correct cavity length and the

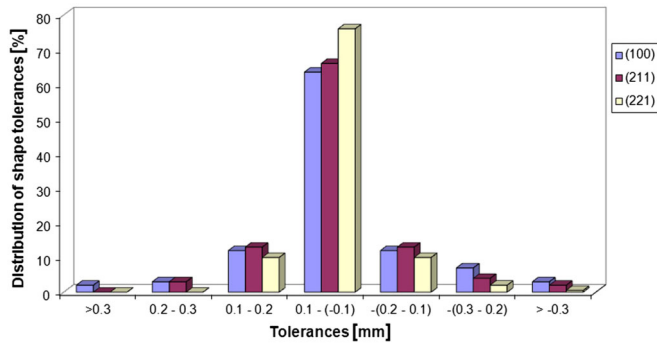


FIG. 10. Dependence of the half-cell shape accuracy on the crystal orientation of the main central crystal. Disks with (100) orientation show bigger deviation from tolerances.

required frequency of the fundamental mode in all nine-cell cavities.

IV. PREPARATION AND RF TESTS

A. Single cell LG cavities, BCP and EP

The main preparation steps for single cell LG cavities were: BCP with more than $80\ \mu\text{m}$ removal, annealing at 800°C for 2 h, approximately $100\ \mu\text{m}$ electropolishing (EP), high pressure water rinsing (HPR) and baking at 130°C for 48 h. EP was carried out at Henkel GmbH, Germany; the BCP was done at RI. Final mechanical and optical quality controls were carried out at DESY.

Investigations with single cell cavities (see also [16]) have shown that relatively high accelerating gradient E_{acc} of approximately $25\text{--}30\ \text{MV/m}$ can be achieved by rather simple BCP treatment $\text{HF}(40\%): \text{HNO}_3(65\%): \text{H}_3\text{PO}_4(85\%)$ at the volume ratio 1:1:2.

Comparison of EP and BCP treatment done on a few large grain single cell cavities has shown that the EP produces better performance. After EP treatment LG single cell cavities reached up to $40\ \text{MV/m}$. More than a $10\ \text{MV/m}$ improvement was found after EP treatment on some previously BCP-treated cavities [16,17]. Figure 11 shows an example of EP superiority compared to BCP. The

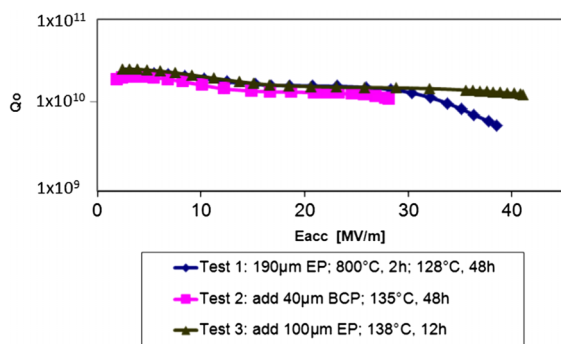


FIG. 11. Unloaded quality factor Q_0 versus accelerating gradient $Q_0(E_{\text{acc}})$ of the LG single cell cavity 1AC4 after EP and BCP treatment.

accelerating gradient of approximately $38\ \text{MV/m}$ previously reached by EP treatment on the cavity 1AC4 became lower by $13\ \text{MV/m}$ after BCP. Repeated EP treatment increased the accelerating gradient again up to $41\ \text{MV/m}$.

B. Nine-cell LG cavities, BCP

BCP treatment was first applied to all DESY nine-cell cavities AC112–AC114, AC151–AC158. The first treatment consisted of the following steps: prior BCP of $100\ \mu\text{m}$ inside and $20\ \mu\text{m}$ outside removal, annealing at 800°C for 2 h, final BCP of $20\ \mu\text{m}$ inside followed by baking at $125^\circ\text{C}\text{--}135^\circ\text{C}$ for 48 h. While the prior BCP treatment for AC112–AC114 was done at DESY, the treatment for cavities AC151–AC158 was done at RI. Inside BCP took place in the RI closed loop system, outside BCP was done by dipping (with protected NbTi-flange surfaces). The final BCP procedure and remaining treatment were carried out at DESY.

The final treatment at DESY started with standard 800°C annealing at a pressure of $<10^{-5}$ mbar for stress release and hydrogen degassing. After tuning to a field flatness of better than 95%, the final inside BCP followed in the closed loop DESY system including ultrapure water rinse and first HPR. Flange and pickup antennas assembly, final six HPR cycles (2 h each), and helium leak check were done in the clean room of class ISO 4. The low temperature baking of the evacuated cavity took place in a heating stand outside of the clean room [18].

The performance of some cavities (in particular AC156, AC152, and AC158) was partially restricted by field emission after the first treatment. Thus, additional HPR was applied to these cavities. HPR included four to six cycles of about 2 h each without additional “baking”.

After the BCP treatment all cavities achieved an accelerating gradient of $24.5\text{--}28.5\ \text{MV/m}$ at 2 K. The performance of most of the cavities was limited by quenches. No evidence of Q disease was observed.

Figure 12 gives the $Q_0(E_{\text{acc}})$ performance at 2 K of 11 LG cavities in their final state before the EP treatment. The specification of the European XFEL, namely $E_{\text{acc}} = 23.6\ \text{MV/m}$ with a quality factor $Q_0 = 1 \times 10^{10}$ was exceeded for all cavities after BCP. In some cases, E_{acc} up to $35\ \text{MV/m}$ was achieved in individual cells during measurements in the different passband modes.

After *in situ* baking, the Q drop at high gradients (in absence of field emission) almost disappeared in agreement with the observed behavior on single cell BCP treated and baked LG cavities [3–5]. For fine grain cavities that were finally BCP treated baking does not change the Q_0 drop much [19].

On the cavities AC113 and AC114 two rf tests were done: first after final BCP without baking and second after additional $20\ \mu\text{m}$ BCP and baking. After *in situ* baking, the Q drop disappeared, but the accelerating gradient was not increased, in contradiction to most reports of observed

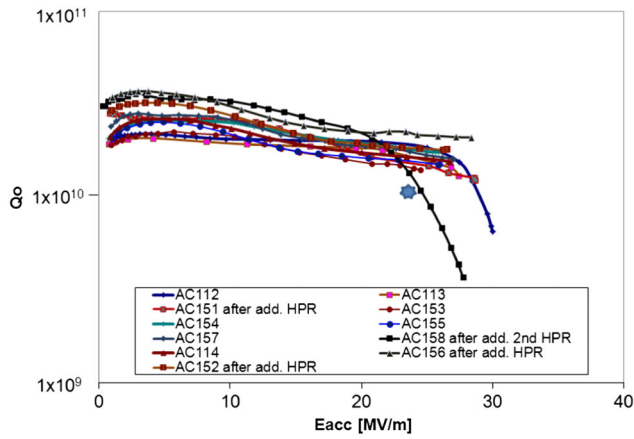


FIG. 12. $Q_0(E_{\text{acc}})$ of the LG cavities AC112–AC114, AC151–AC158 at 2 K after BCP. Test after prior 100 μm BCP, annealing at 800°C for 2 h, final BCP of 20 μm , and baking at 130°C for 48 h. The star shows the XFEL requirements. AC112 was not baked; AC113 and AC114 are baked after additional 20 μm BCP; AC158 demonstrated after 2nd HPR still field emission.

behavior on single cell BCP-treated and baked LG cavities [3–5].

After additional HPR only one cavity (AC158) was restricted by enhanced field emission and barely fulfilled the XFEL requirements. The cavity AC112 was not baked and therefore demonstrates a Q slope from 27 to 30 MV/m. As mentioned above, the steps on grain boundaries have been ground on two cavities AC155 and AC156. Both ground cavities do not show any deviation compared to other cavities.

It is interesting to compare performance of LG cavities and similar treated cavities from polycrystalline niobium (BCP treated and 800°C annealed). Several cavities were treated that way during the TTF project at DESY in the 1990s. The comparison shows that the average value of E_{acc} for LG cavities is of approximately 5 MV/m higher than the average E_{acc} of conventional cavities. Plausible reasons for such differences could lay in the difference in the thermal conductivity caused by phonon peak, or in the mirrorlike shiny internal surface of BCP-treated LG cavities (see also [17]).

C. Nine-cell LG cavities, EP

After the BCP treatment and rf tests, the restrictions of possible material removal during subsequent EP treatment with respect to frequency and tolerable length were estimated. Consequently, two different procedures were applied [18].

(i) For six cavities a main EP at DESY [20] of about 60–70 μm was done, followed by an ethanol rinse, an additional standard 800°C firing for 2 h at a pressure of $<10^{-5}$ mbar, and a final EP. Before the final EP, the field flatness was checked again and, if necessary, tuned to better than 95%. After final EP of approximately 50 μm ,

the ethanol rinse [21], final six HPR cycles, and baking at 120°C were done. Most treatment procedures took place in the clean room of class ISO 4.

(ii) Two cavities (AC151, AC155) were unsuitable for the main EP. Their tolerable length in the cryomodule at the operating frequency would be exceeded due to the additional removal. Therefore, after tuning only the final EP of approximately 50 μm was done, followed by the ethanol rinse, final six HPR cycles, and 120°C baking.

The parameters of the baking procedure after EP treatment were identical to the parameters after BCP treatment.

The vertical rf test of 11 LG cavities has shown accelerating gradients 31–45.5 MV/m at Q_0 values above 10^{10} limited mostly by breakdown. Some cavities suffer a bit from a weak field emission. E_{acc} of only one cavity AC151 was limited by a strong field emission. No difference in maximum gradient between 1.8 and 2 K was detected. No evidence of Q disease was observed. Figure 13 gives the $Q_0(E_{\text{acc}})$ performance at 2 K of these cavities.

Enhancing the acceleration gradient typically by more than 10 MV/m after EP regarding to BCP can be seen on most cavities (compare Figs. 12 and 13).

A degradation of E_{acc} after EP from 28 to 14 MV/m was observed only for one cavity AC114. The acceleration gradient of the individual cells was dramatically reduced from 28–35 MV/m to 15–22 MV/m as well. For π mode, the quench was found by temperature mapping (T mapping) in cell 2 above and near the equator [6]. In addition, many other smaller hot spots were found in several cells. Large groups of craters with a size up to 0.5 mm on the entire inner surface of all cells were found by optical inspection with high resolution camera on the EP-treated cavity. It appears that the craters could be responsible for the performance degradation in many cells.

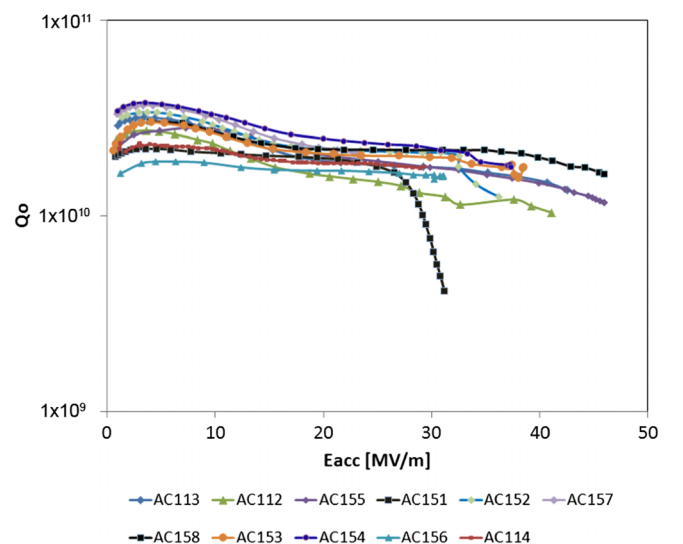


FIG. 13. Final $Q_0(E_{\text{acc}})$ performance of the LG cavities AC112–AC114, AC151–AC158 at 2 K after EP.

The cause of such craters is now being discussed worldwide and seems not be specific to LG cavities only (see for example [22]). It is difficult to say whether the LG grain surface behaves in an unusual manner during EP treatment compared to fine grain. It is possible that some imperfections were already present before EP and became larger with EP, if EP does not work properly. Unfortunately, the optical inspection data after BCP treatment are missing.

The cavity AC114 was additionally treated by centrifugal barrel polishing (CBP) at FNAL. Around 120–130 μm was removed by CBP and approximately 30 μm removed by subsequent EP. The quality of the inside surface was significantly improved; the craters mostly vanished so that the power rf test at FNAL showed an accelerating gradient of 29 MV/m. This curve is inserted in Fig. 13.

Figure 13 shows that gradients of 45 MV/m were achieved in two LG cavities AC155 and AC158 (the detailed measurements done on these two cavities is described in [18]). This E_{acc} value is equivalent to magnetic

surface fields of 192 mT. Passband mode measurements up to 213 mT for individual cells were observed. This is in agreement with the highest magnetic surface fields measured in other labs [23] and among the highest fields ever measured in multicell cavities. Finally, after additional six HPR, a rotating T mapping was done on the cavity AC158. The break down position was found in π mode in cell 8 near the equator at 170° at 44 MV/m with $Q_0 = 1.4 \times 10^{10}$.

The cavities AC155 and AC156 with ground grain boundaries achieved accelerating gradients of 45.5 and 31 MV/m, respectively. So far, no clear influence of the grinding of grain boundaries on the cavity performance can be concluded.

Another interesting aspect of LG cavity behavior, which has to be stressed, is the rather high unloaded quality factor Q_0 , after EP treatment, even at high gradients. As seen in Fig. 14(a), the Q_0 reaches up to 4×10^{10} at 2 K at moderate accelerating gradients. Figure 14(a) compares the Q_0 of 11 EP-treated LG cavities with Q_0 of 15 XFEL prototype cavities (AC115–AC129) built at RI and treated at DESY according to an XFEL recipe [24]. As it can be clearly seen, the Q_0 value for LG cavities is approximately 25%–30% larger than for conventional fine grain cavities and this indicates the high potential of LG cavities in applications requiring high Q_0 , for example in continuous wave (CW) applications. Superiority of the Q_0 of LG cavities after BCP treatment is less pronounced [Fig. 14(b)].

V. SUMMARY AND OUTLOOK

It was shown that it is feasible to build not only single cell, but also nine-cell cavities from LG material without significant difficulties or special problems. The accelerating gradients by BCP treatment up to 30 MV/m in the π -mode measurement ($B_p = 110$ – 130 mT) and up to 35 MV/m in the passband measurement is achieved in a stable and reproducible manner for all 11 nine-cell LG tesla shaped cavities. Accelerating gradients on the level of 35–45 MV/m can be achieved by applying EP treatment.

Why does the EP treatment allow reaching better performance as BCP? The surface quality of large grains is comparable for BCP and EP treatment. The surface roughness of the BCP-treated large grains depends on crystal orientation, but is on the same level as EP-treated fine grain material (hundreds of nm). This is shown in Fig. 15 and Table I as characterization results of BCP done on samples of approximately 50 mm diameter separated from the disks central crystals before deep drawing of half-cells for cavities AC151–AC158 (approximately 80 μm removed by BCP).

It seems that the difference between BCP and EP treatment of LG cavities is caused by the grain boundaries. For better understanding of this difference, it would be reasonable to take into consideration the behavior of the single

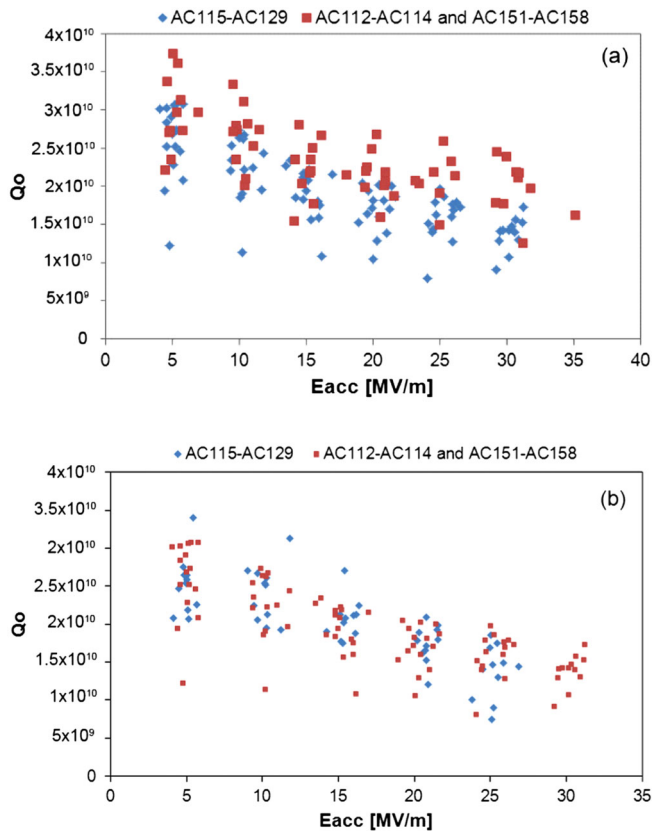


FIG. 14. (a) Comparison of unloaded quality factor Q_0 at 2 K for 11 EP-treated LG cavities (red) with Q_0 at 2 K of XFEL prototype cavities (AC115–AC129, best result) treated according to XFEL recipe (partly final EP and partly BCP flash [24] were applied) (blue). (b) Comparison of unloaded quality factor Q_0 at 2 K for 11 BCP-treated LG cavities (red) with Q_0 at 2 K of XFEL prototype cavities (AC115–AC129, best result) treated according XFEL recipe (partly final EP and partly BCP flash [24] were applied) (blue).

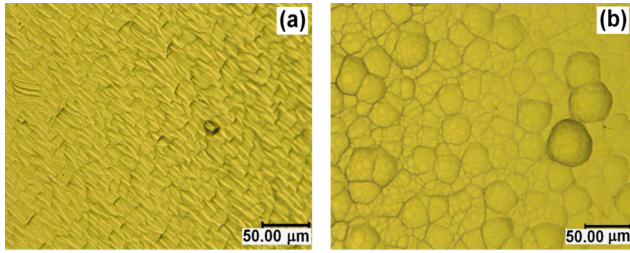


FIG. 15. Surface of the central crystals of cavities AC154 and AC158 [orientation (211)] (a). Surface of the central crystals for cavities AC151, AC152, and AC153 [orientation (100)] (b).

crystal cavities (cavities without grain boundaries at all). A fabrication method for single crystal cavities was proposed and few single cell single crystal cavities have been produced recently [17,25]. It was demonstrated that for BCP-treated single crystal cavities a similar performance as after EP treatment in LG cavities, namely, an accelerating gradient on the level of 40 MV/m, is reachable. This allows concluding that probably the main difference between BCP and EP in LG cavities lays in the grain boundaries. The BCP treatment creates the steps on grain boundaries. The step height depends on the crystallographic orientation of the neighboring grains and can be different as Figs. 16(a) and 16(b) demonstrate.

Evidently, the steps on the grain boundaries after BCP on LG material restrict the accelerating gradient at 25–30 MV/m.

The most reasonable explanation of that gives the model of magnetic field enhancement at grain boundary edges, which has a geometrical nature [23,26]. The magnetic field enhancement in this model depends not only on the step height, but also on step angle and corner radius [26].

EP, contrary to BCP, diminishes the steps on grain boundaries. Optical inspection carried out by a high resolution camera supports this [27] [Figs. 17(a) and 17(b)]. As can be seen in the figures, the steps on grain boundaries of BCP-treated cavities do not disappear completely after EP, but become much smoother.

From this point of view, the grinding away of the big (up to 0.5 mm) steps on the deep drawn half-cells could have only small influence on performance, because the 120 μm BCP treatment of cavities creates the steps on grain

TABLE I. Surface roughness R_a (arithmetic average of absolute values), R_z (average distance between the highest peak and lowest valley in each sampling length), and R_q (root mean squared values) of samples of the central crystals with different orientations.

	(211)	(221)	(100)	(111)	(110)
R_a , μm	0.15	0.2	0.24	0.35	0.36
R_z , μm	0.57	0.85	0.89	1.7	1.94
R_q , μm	0.19	0.25	0.3	0.42	0.44

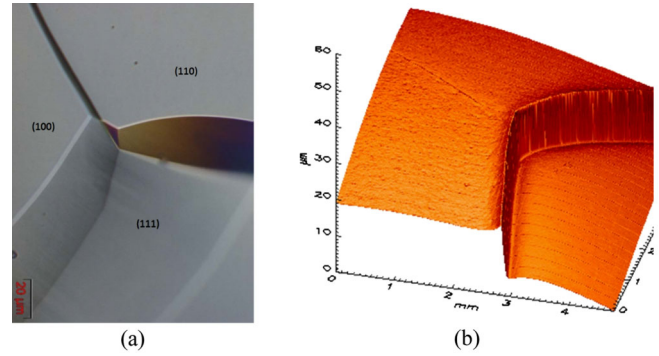


FIG. 16. Light microscope image of the grain boundary triple junction of LG Nb after 100 μm BCP on the previously mechanically polished sample (a). Orientation type is shown on grains. Atom force microscope image of the same area (b). Steps on grain boundaries are within 1.5–15 μm for this orientation constellation.

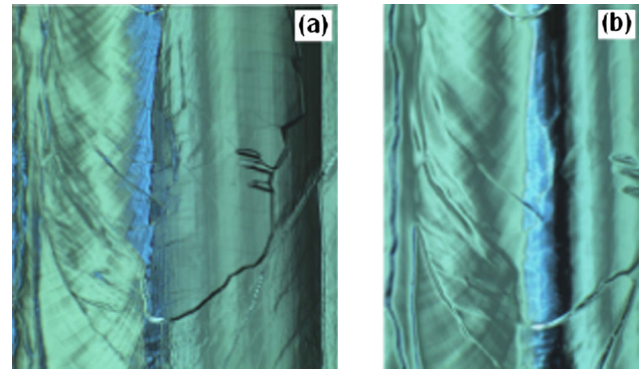


FIG. 17. Example of sharp grain boundary in AC158 after BCP treatment (a) and the same grain boundary smoothed by EP treatment (b).

boundaries again and subsequent EP makes them smoother another time.

As mentioned above, in several cases a field emission load was observed in LG cavities. One can ask if large or sharp steps on grain boundaries are critical for that. The investigation [28] has shown that the onset of field emission is shifted even to higher electrical fields in LG samples compared to fine grain ones; the field emitters mostly appeared close to grain boundaries. However, our LG cavities do not have grain boundaries in the iris area vulnerable for field emission due to the large single crystal in the disk center.

On the other hand, some slip lines were observed in deep drawn half-cells and they probably could be field emission sources [29] (see Fig. 18). Because of poor statistics, it is difficult to conclude whether the LG cavities have any disadvantages concerning the field emission phenomena.

The complete chain of the LG cavity technique beginning from material production and ending with cavity installation into a cryomodule was successfully tested. Cavity AC112 was installed into cryomodule 3***, cavity

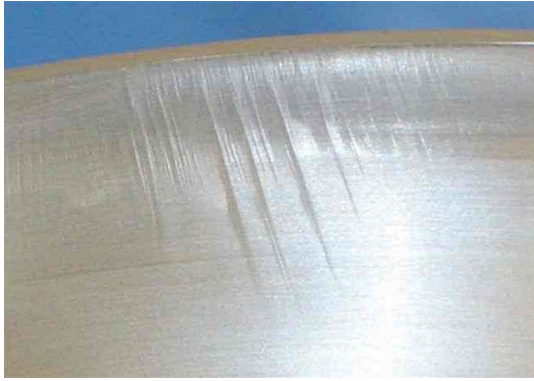


FIG. 18. Slip lines of the crystal on a half-cell after deep drawing.

AC113 was installed in cryomodule PXFEL1 in the FLASH accelerator at DESY.

Both cavities are currently operational in the machine and contributing to the beam energy of 1.25 GeV. Production of a complete XFEL cryomodule containing

only LG cavities is planned. Work on integration into a helium tank of cavities AC151–AC158 is currently under way.

Unfortunately, the industry is not ready yet for mass production of the LG material. However, there is no doubt that the high potential of LG cavities will be taken into consideration for future accelerators. Considering the simple preparation procedure and small scattering in the performance, BCP-treated LG cavities can be recommended for applications in accelerators with medium requirements for accelerating gradients. High quality factor Q_0 and high accelerating gradient E_{acc} of EP-treated LG cavities can be, in particular, reasonable for CW application and for the ILC project.

Based on our experience and discussions during the past few years on workshops and conferences [1,2,30], the advantages and disadvantages of LG cavities are summarized in Table II.

It is worthwhile to mention some efforts that possibly can reduce the weight of the last two “Contra” points. Using special electron beam melting parameters the size of

TABLE II. Advantages and disadvantages of LG cavities.

Pro	Contra
1. LG disks are more cost effective as fine grain sheets (32% according to the estimate for XFEL preseries cavities).	1. LG is currently not usable for mass production. For example, the industry is not in a position to produce the required amount of approximately 20 tons of LG material for the European XFEL in 2 years.
2. The wire saw procedure allows getting high surface quality and thickness tolerances in disks.	2. Only one company has industrial experience for LG cavity production.
3. Increased thermal conductivity close to 2 K due to phonon effect helps to lead the heat away from hot spots.	3. Mechanical fabrication works, but needs additional effort due to a not sufficiently precise shape of half-cells (clamping for trimming, trimming accuracy, frequency measurement, assembling of half-cells for welding).
4. Simplified quality control is possible. No danger that during many production steps from ingot to sheet the material will be polluted (no RRR degradation). Eddy current scanning is avoidable.	
5. Accelerating gradient of 25–30 MV/m can be reached by simple preparation with BCP only. The best result of 45 MV/m reached after EP on two cavities is a world record for this cavity type.	
6. Onset of Q drop in large grain cavities is typically at 10% higher accelerating gradients.	
7. It is sufficient to bake the BCP-treated cavity at 120°C for only 12–24 h.	
8. The complete chain of the LG cavity technique beginning with material production and ending with cavity installation into a cryomodule is proven.	
9. The quality factor Q_0 of EP-treated LG cavities is approximately 25%–30% larger compared to similar fine grain cavities.	
10. The wire saw method caused much less stress at the surface of the disk compared to rolled sheets (reduces influence of the damage layer on performance).	

large grains in the ingot can be reduced [31]. Minimization of the anisotropic behavior during deep drawing and therefore better shape accuracy could be expected in this case.

ACKNOWLEDGMENTS

We would like to thank our colleagues B. van der Horst, I. Jelezov, L. Lilje, M. Pekeler, B. Spaniol, and N. Steinhau-Kühl for their support of this work. Many thanks to C. Cooper for CBP treatment, EP and subsequent rf test of the cavity AC114 at FNAL.

-
- [1] *Proceedings of the International Niobium Workshop, 2006, Araxa, Brazil*, AIP Conf. Proc. No. 927, edited by G. Myneni, T. Carneiro, and A. Hutton (AIP, New York, 2007).
- [2] *Proceedings of the International Niobium Workshop, 2006, Araxa, Brazil*, AIP Conf. Proc. No. 1352, edited by G. Myneni, G. Ciovati, and M. Stuart (AIP, New York, 2010).
- [3] P. Kneisel, G. R. Myneni, G. Ciovati, J. Sekutowicz, and T. Carneiro, in *Development of Large Grain / Single Crystal Niobium Cavity Technology at Jefferson Lab*, AIP Conf. Proc. No. 927 (AIP, New York, 2007), pp. 84–97.
- [4] P. Kneisel, G. R. Myneni, G. Ciovati, J. Sekutowicz, and T. Carneiro, in *Proceedings of the 12th Workshop on RF Superconductivity*, Ithaca, NY, 2005, MoP09.
- [5] P. Kneisel, *Progress on Large Grain and Single Grain Niobium*, SRF07, Beijing, 2007, TH102.
- [6] W. Singer, S. Aderhold, J. Iversen, G. Kreps, L. Lilje, A. Matheisen, X. Singer, H. Weise, M. Pekeler, J. Schwellenbach, F. Scholz, B. Spaniol, and E. Stiedl, in *Proceedings of the 23rd Particle Accelerator Conference, Vancouver, Canada, 2009* (IEEE, Piscataway, NJ, 2009), TU5PFP054.
- [7] H. Umezawa, *Niobium Production at Tokyo Denkai*, AIP Conf. Proc. No. 1352 (AIP, New York, 2010), pp. 79–83.
- [8] W. Singer *et al.*, *Large Grain Superconducting RF Cavities at DESY, International Niobium Workshop, 2006, Araxa, Brazil* (AIP, New York, 2007), p. 123–132.
- [9] A. Ermakov, I. Jelezov, X. Singer, W. Singer, G. B. Viswanathan, V. Levit, H. L. Fraser, H. Wen, and M. Spiwek, *J. Phys. Conf. Ser.* **97**, 012014 (2008).
- [10] F. Koechlin and B. Bonin, *Supercond. Sci. Technol.* **9**, 453 (1996).
- [11] W. Wasserbäch, *Philos. Mag. A* **38**, 401 (1978).
- [12] P. Dhakal, G. Ciovati, P. Kneisel, and R. Myneni, *Superconducting DC and RF Properties of Ingot Niobium*, 15th International Conference on RF Superconductivity, Chicago, Illinois, 2011, THP0057, p. 130.
- [13] Umformtechnik. *Handbuch für Industrie und Wissenschaft, Band 1* (Springer-Verlag, Berlin, 1984).
- [14] A. Schmidt, A. Brinkmann, J. Iversen, A. Matheisen, D. Reschke, M. Schäfer, W. Singer, V. Sousa, J. Tiessen, and D. Vermeulen, TTC Report No. 2010-01, p. 11.
- [15] G. Kreps, D. Proch, and J. Sekutowicz, *Half-cell and Dumb-bell Frequency Testing for the Correction of the TESLA Cavity Length*, in *Proceedings of the 9th Workshop on RF Superconductivity*, Santa Fe, New Mexico, 1999, p. 499–504.
- [16] A. Brinkmann, J. Iversen, D. Reschke, W. Singer, X. Singer, K. Twarowski, and J. Ziegler, in *Proceedings of SRF07*, Beijing, 2007.
- [17] W. Singer *et al.*, in *Proceedings of the 2007 Particle Accelerator Conference*, Albuquerque, New Mexico (IEEE, New York, 2007), THOAKI01.
- [18] D. Reschke *et al.*, *Results on Large Grain Nine-cell Cavities at DESY: Gradients up to 45 MV/m after Electropolishing*, SRF2011, Chicago, USA.
- [19] D. Reschke, L. Lilje, and H. Weise, in *Proceedings of the SRF 2009*, Germany, Berlin, 2009.
- [20] N. Steinhau-Kühl *et al.*, in *Proceedings of the Workshop on RF Superconductivity 2003*, Lübeck/Travemünde, Germany (2003), TuP46.
- [21] B. v. d. Horst *et al.*, in *Proceedings of the Workshop on RF Superconductivity 2007*, Beijing, China, 2007, TUP30.
- [22] W. Singer, X. Singer, S. Aderhold, A. Ermakov, K. Twarowski, R. Crooks, M. Hoss, F. Schölz, and B. Spaniol, *Phys. Rev. ST Accel. Beams* **14**, 050702 (2011).
- [23] H. Padamsee, *RF Superconductivity* (Wiley-VCH, Weinheim, Germany, 2009), p. 448.
- [24] W. Singer *et al.*, in *IPAC2010*, Kyoto, Japan, THOARA02.
- [25] P. Kneisel, G. Ciovati, W. Singer, X. Singer, D. Reschke, and A. Brinkmann, in *Proceedings of the 11th European Particle Accelerator Conference, Genoa, 2008* (EPS-AG, Genoa, Italy, 2008), MOPP136, p. 877–879.
- [26] H. Padamsee, J. Knobloch, and T. Hays, *RF Superconductivity for Accelerators* (Wiley-VCH, Weinheim, Germany, 2008), 2nd ed., p. 521.
- [27] S. Aderhold, in *Proceedings of SRF 2011*, Chicago, 2011, WEIOB05.
- [28] A. Dangwal Pandey, G. Mueller, D. Reschke, and X. Singer, *Phys. Rev. ST Accel. Beams* **12**, 023501 (2009).
- [29] X. Singer, J. Iversen, W. Singer, K. Twarowski, B. Spaniol, F. Schölz, H.-G. Brokmeier, in *Proceedings of Workshop on RF Superconductivity*, Chicago, 2011, THPO053.
- [30] G. Ciovati and G. R. Myneni, in *Proceedings of Workshop on RF Superconductivity*, Chicago, 2011.
- [31] B. Spaniol (private communication).